European Journal of Medicinal Chemistry 90 (2015) 507–518

Contents lists available at ScienceDirect

European Journal of Medicinal Chemistry

journal homepage: http://www.elsevier.com/locate/ejmech

Original article

Synthesis and structure–activity-relationship studies of thiazolidinediones as antiplasmodial inhibitors of the *Plasmodium falciparum* cysteine protease falcipain-2

Rajni Kant Sharma [a], Yassir Younis [a], Grace Mugumbate [a], Mathew Njoroge [a], Jiri Gut [b], Philip J. Rosenthal [b], Kelly Chibale [a, c, d, *]

[a] Department of Chemistry, University of Cape Town, Rondebosch 7701, South Africa
[b] Department of Medicine, University of California, San Francisco, CA 94143, USA
[c] Institute of Infectious Disease and Molecular Medicine, University of Cape Town, Rondebosch 7701, South Africa
[d] South African Medical Research Council, Drug Discovery and Development Unit, University of Cape Town, Rondebosch 7701, South Africa

ARTICLE INFO

Article history:
Received 4 August 2014
Received in revised form
25 November 2014
Accepted 29 November 2014
Available online 2 December 2014

Keywords:
Antiplasmodial agents
Thiazolidinone
Falcipain-2

ABSTRACT

Following a structure-based virtual screening, a series of 2,4 thiazolidinediones was synthesized in order to explore structure activity relationships for inhibition of the *Plasmodium falciparum* cysteine protease falcipain-2 (FP-2) and of whole cell antiparasitic activity. Most compounds exhibited low micromolar antiplasmodial activities against the *P. falciparum* drug resistant W2 strain. The most active compounds of the series were tested for *in vitro* microsomal metabolic stability and found to be susceptible to hepatic metabolism. Subsequent metabolite identification studies highlighted the metabolic hot spots. Molecular docking studies of a frontrunner inhibitor were carried out to determine the probable binding mode of this class of inhibitors in the active site of FP-2.

1. Introduction

Malaria is a major cause of morbidity and mortality. According to the 2012 World Health Organization (WHO) report, malaria is responsible for an estimated 500,000–900,000 deaths each year, especially among children and pregnant women [1]. *Plasmodium falciparum*, the most virulent human malaria parasite and *Plasmodium vivax* are responsible for more than 95% of malaria cases in the world. In light of established and continuing development of resistance of *P. falciparum* to most antimalarial drugs, the identification and characterization of novel antimalarial chemotypes is an important priority [2–4].

The *P. falciparum* cysteine protease falcipain-2 (FP-2), is a key enzyme in the life cycle of *P. falciparum* since it is involved in the digestion of host haemoglobin in the digestive vacuole of the parasite, providing amino acids for its survival and development [5]. This makes FP-2 an attractive target for antimalarial drug design. Hence, to date, many chemotypes have been identified as FP-2 inhibitors [6–20]. In an effort to identify potential antimalarial inhibitors of FP-2, structure-based virtual screening of the ZINC database, which contains more than 13 million drug like compounds, was previously carried out. A total of 32 high ranked compounds were purchased from the SPECs chemical database (www.specs.net), and 14 compounds with activity against the drug resistant *P. falciparum* W2 strain and FP-2 were identified [21]. Amongst these structures is a thiazolidine-2,4-dione (TZD) derivative, **TZD 4** (Fig. 1), which exhibited modest activity against FP-2 (IC_{50} = 25.5 μM) and *P. falciparum* (EC_{50} = 0.45 μM). Compound **TZD 4** was selected for subsequent hit validation through resynthesis and biological retesting. Although thiazolidinedione derivatives have been reported to have antimicrobial, anti-proliferative, anti-viral, anti-convulsant, anti-inflammatory and anti-cancer activities [22–28], to our knowledge their antiplasmodial activity has not previously been studied.

In this paper we report the synthesis and structure–activity-relationship studies around the thiazolidinedione core. In addition, we report microsomal metabolic stability profiling and molecular docking studies of frontrunner compounds.

* Corresponding author. Department of Chemistry, University of Cape Town, Rondebosch 7701, South Africa.
E-mail address: Kelly.Chibale@uct.ac.za (K. Chibale).

http://dx.doi.org/10.1016/j.ejmech.2014.11.061
0223-5234/

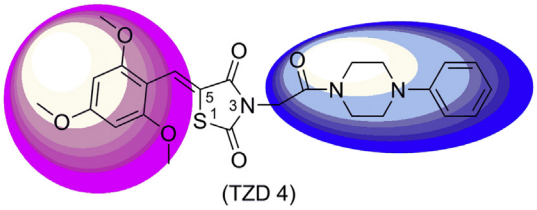

Fig. 1. Chemical structure of the thiazolidine-2,4-dione derivative **TZD 4** and two sites of modifications as depicted by blue and pink rings. (For interpretation of the references to colour in this figure legend, the reader is referred to the web version of this article.)

2. Results and discussion

2.1. Chemistry

The target compounds **TZD 4**, **4a**–**t** were synthesized using an efficient 3-step synthetic route (Scheme 1; a). The synthesis commenced with commercially available 1-phenyl piperazine **1**, which was reacted with chloroacetyl chloride in the presence of triethylamine at 0 °C for 1 h to give 2-chloro-1-(4-phenylpiperazin-1-yl)ethanone **2**. This intermediate and 2,4-thiazolidinedione **5**, in acetone under basic conditions, were heated for 24 h to yield the key intermediate **3**, which was reacted with appropriate substituted benzaldehydes using the Knoevenagel condensation reaction under microwave irradiation to obtain a library of C-5 substituted analogues [29]. By fixing the trimethoxyphenyl substituent at the C-5 position and varying substituents at the N-3 position, two sets of the target compounds **9a**–**j** and **11a**–**i** were synthesized as shown in (Scheme 1; b, c). For the synthesis of analogues **9a**–**j**, the free acid intermediate **7** was prepared and subjected to a Knoevenagel condensation reaction with 2,4,6-trimethoxybenzaldehyde to obtain the key intermediate **8** as shown in Scheme 1; b. The intermediate **8** was reacted with appropriate substituted piperazines to deliver the target compounds **9a**–**j** in moderate yield. The second set of N-3 linked analogues **11a**–**i** was synthesized by a similar synthetic protocol as described in Scheme 1; c.

2.2. Biological evaluation

The activities of all synthesized compounds were determined *in vitro* against FP-2 and the chloroquine resistant W2 strain of *P. falciparum* (Tables 1 and 2). E-64, chloroquine and artesunate were included as controls in all experiments. A first set of analogues was designed in order to explore the SAR around the trimethoxyphenyl group of **TZD 4** at position 5, as shown in Table 1. In this work, the resynthesised **TZD 4** exhibited relatively weak activity

Table 1
In vitro antiplasmodial activities of **TZD 4**, **4a**–**v** compounds against FP-2 and *P. falciparum* (IC_{50} μM).

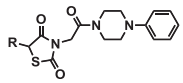

Cpd	R	*P. falciparum* EC_{50} (μM)	FP2 IC_{50} (μM)	Cpd	R	W2 EC_{50} (μM)	FP2 IC_{50} (μM)
TZD 4		0.88	>50	**4k**		>10	35.28
4a		4.65	>50	**4l**		>10	44.97
4b		>10	>50	**4m**		>10	33.25
4c		>10	>50	**4n**		>10	>50
4d		>10	>50	**4o**		>10	>50
4e		>10	13.44	**4p**		>10	>50
4f		>10	18.04	**4q**		>10	>50
4g		>10	15.80	**4r**		>10	45.71
4h		>10	23.88	**4s**		>10	45.33
4i		>10	23.89	**4t**		>10	38.80
4j		>10	35.28	**3**	H	>10	>50
ART		0.019		ART		0.019	
CQ		0.033		CQ		0.033	
E64			0.047	E64			0.047

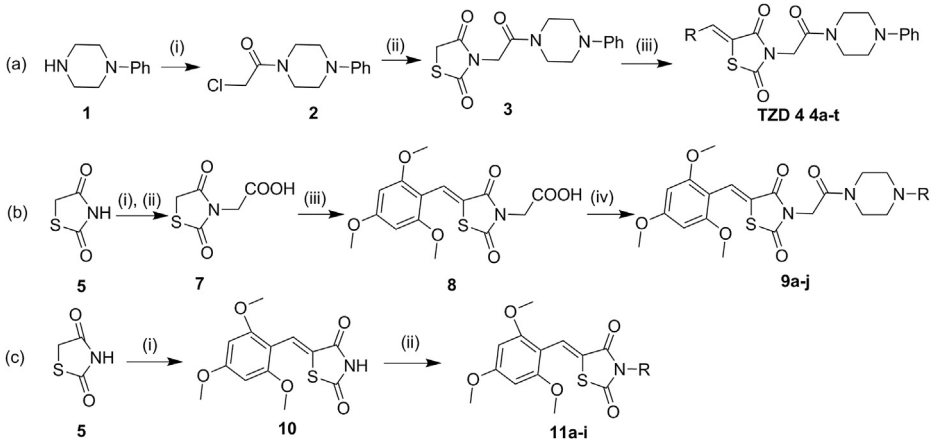

Scheme 1. Reagents and conditions: (a) (i) chloroacetyl chloride, Et_3N, DCM, 0 °C, 1 h; (55%) (ii) 2,4 thiazolidinedione, K_2CO_3, acetone, 60–70 °C, 24 h; (52%) (iii) substituted aldehydes, NH_4OH, toluene, MW, 170 °C, 20–30 min; (b) (i) bromoacetylmethylester, NaH, DMF, 0 °C–25 °C, 24 h; (ii) HBr (48%), 100 °C, 4 h; (52%) (iii) 2,4,6-trimethoxybenzaldehyde, piperidine, AcOH, 50 °C, 5 h; (69%) (iv) substituted piperazines, EDCI, $HOBt{\cdot}H_2O$, DIPEA, DMF, 0 °C–25 °C, 24 h; (c) (i) 2,4,6-trimethoxybenzaldehyde, piperidine, AcOH, 50 °C, 5 h; (76%) (ii) alkyl/aryl halides, NaH, DMF, 0 °C–25 °C, 14 h. For complete structure see Tables 1–2.

Table 2
In vitro antiplasmodial activities of **8**, **9a**–**j**, **10** and **11a**–**i** compounds against the W2 (EC_{50} μM) strain and FP-2 enzyme of *P. falciparum* (IC_{50} μM).

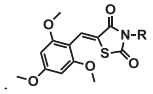

Cpd	R	W2 EC_{50} (μM)	FP2 IC_{50} (μM)	Cpd	R	W2 EC_{50} (μM)	FP2 IC_{50} (μM)
8	CH_2CO_2H	>10	>50	**10**	H	>10	47.84
9a		5.28	>50	**11a**	CH_3	>10	>50
9b		>10	>50	**11b**	CH_2CH_3	>10	>50
9c	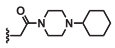	3.56	>50	**11c**		>10	36.24
9d	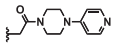	1.6	>50	**11d**		8.88	43.35
9e	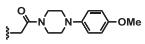	1.21	>50	**11e**		>10	29.08
9f	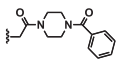	4.70	33.75	**11f**		8.75	>50
9g	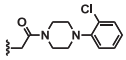	1.11	12.64	**11g**	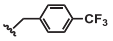	>10	>50
9h	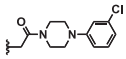	0.55	16.25	**11h**		>10	>50
9i	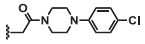	1.43	11.23	**11i**		>10	29.08
9j	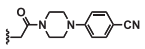	3.97	12.24				
ART		0.019		ART		0.019	
CQ		0.033		CQ		0.033	
E64			0.047	E64			0.047

Cpd: compound.

against *P. falciparum* and FP-2, with EC_{50} = 0.88 μM and IC_{50} > 50 μM respectively, compared to previously reported activities [21]. Removal of one or two methoxy substituents in **TZD 4**, did not enhance inhibition of FP-2 as shown by activities of **4a**–**c** (IC_{50} > 50 μM). However, introduction of strong electron withdrawing groups (OCF_3, CF_3) at the *para* position of the phenyl ring resulted in improved enzyme inhibitory activity for **4e** (IC_{50} = 13.44 μM) and **4f** (IC_{50} = 18.04 μM). Significantly reduced enzyme activity was observed on introduction of *para* halogen or di-halogen substitutions on the phenyl ring as in **4d**, **4o**, **4n** and **4p** (IC_{50} > 50 μM). Interestingly, *ortho* halogen substitutions resulted in increased enzyme inhibitory activity, as exemplified by **4g** (IC_{50} = 15.80 μM) and **4h** (IC_{50} = 23.88 μM). The *meta* methyl substituted compound **4s** displayed modest potency (IC_{50} = 45.33 μM), but replacement of the methyl group with isopropyl **4i** led to marked improvement in potency (IC_{50} = 23.89 μM). However, no improvement in activity against *P. falciparum* was observed.

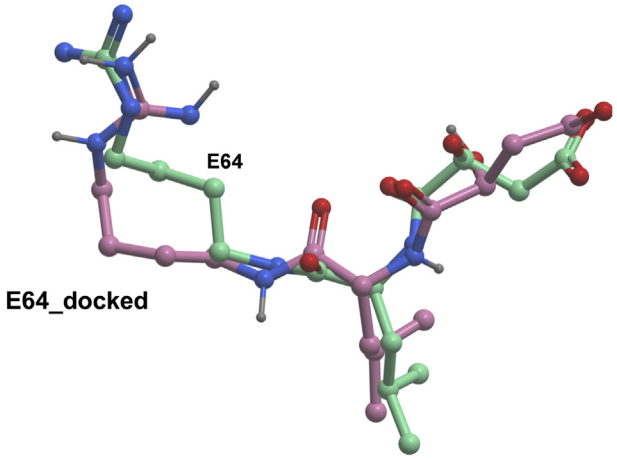

Fig. 2. Comparison of the docked (pink) and crystal structure (green) conformations of E64. (For interpretation of the references to colour in this figure legend, the reader is referred to the web version of this article.)

The next phase of SAR exploration was directed at optimising position 3 of the thiazolidinedione core while fixing the trimethoxyphenyl group, as shown in Table 2. Removal or replacement of the right hand side of compound **TZD 4** with aliphatic alkyl moieties or substituted benzyl groups revealed no significant improvement in FP-2 inhibitory activity as in **8**, **11a**, **11b** and **11f**–**h** (IC_{50} > 50 μM). Interestingly, introducing a chloro substituent at the *ortho*, *meta* and *para* positions of the phenyl ring led to significant improvement in enzyme inhibitory and W2 activities, as demonstrated by **9g** (FP-2 IC_{50} = 12.64 μM; W2 EC_{50} = 1.11 μM), **9h** (FP-2 IC_{50} = 16.25 μM; W2 EC_{50} = 0.55 μM), and **9i** (FP-2 IC_{50} = 11.23 μM; W2 EC_{50} = 1.43 μM). Similarly, introducing the electron withdrawing cyano group at the *para* position of the phenyl ring resulted in moderate enzyme inhibitory and whole cell potency, as demonstrated by compound **9j** (FP-2 12.24 μM; W2 3.97 μM), while compound **9e** (FP-2 IC_{50} > 50 μM; W2 EC_{50} = 1.21 μM) with the *para*

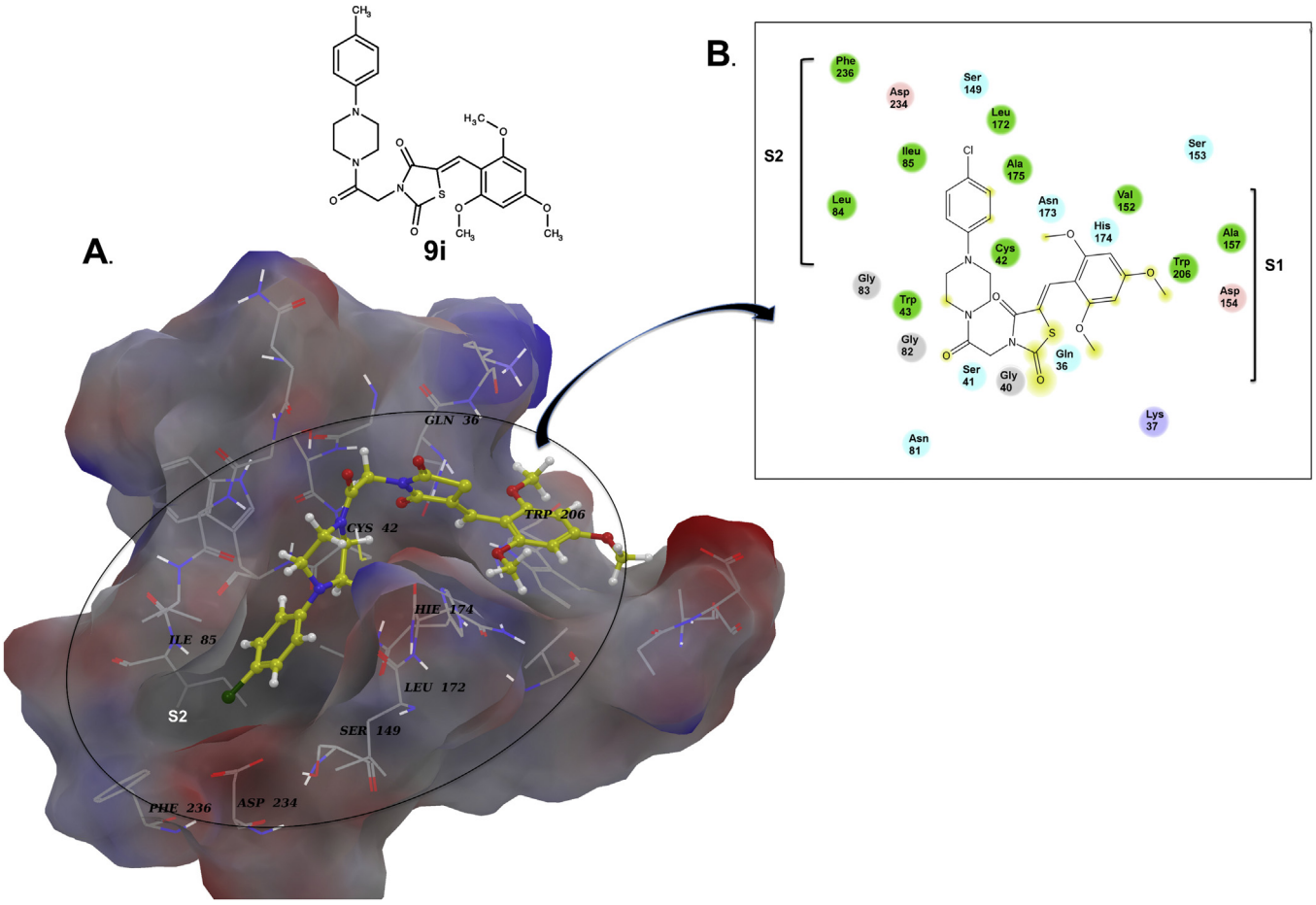

Fig. 3. Binding mode of compound **9i** (2D structure) in binding pocket of FP2. A) Electrostatic potential (red – negative and blue – positive) surface structure of FP-2 showing subsites S1, S2, and S3. The yellow sticks and balls (coloured by atom type) depict the docked conformation of compound **9i** in the binding site of FP-2. C) 2D representation of interactions between compound **9i** and some amino acid residues in S1 and S2 subsites of FP-2 (green – hydrophobic, cyan-polar, pink ionic residues and yellow shows solvent exposed atoms in the ligand). (For interpretation of the references to colour in this figure legend, the reader is referred to the web version of this article.)

methoxy substituent showed no enzyme inhibition at the highest concentration tested, but retained whole cell activity (W2 EC_{50} = 1.21 μM). Replacement of the phenyl ring with cyclohexyl and 4-pyridyl substituents also resulted in compounds with no enzyme inhibitory activity at the highest concentration tested, but antiplasmodial activity, as exemplified by compounds **9c** (FP-2 IC_{50} > 50 μM; W2 EC_{50} = 3.56 μM), **9d** (FP-2 IC_{50} > 50 μM; W2 EC_{50} = 1.6 μM). Thus, a lack of correlation between FP2 inhibitory activity and whole cell activity was evident, suggesting that compounds were acting against other yet unknown plasmodial targets.

Table 3
Results from the *in vitro* microsomal stability of **TZD 4**, **9g**, **9h**, **9i**, **9j**.

Compound	LM species	% Remaining	Predicted half-life (min)	Solubility (μM)	
				pH 2	pH 6.5
TZD 4	Human	5.4	7.1	<5	<5
	Rat	4.3	6.6		
	Mouse	6.1	7.4		
9g	Human	34.0	19.3	<5	<5
	Rat	20.2	13.0		
	Mouse	1.7	5.1		
9h	Human	12.9	10.2	<5	<5
	Rat	31.1	17.8		
	Mouse	3.0	5.9		
9i	Human	47.2	27.7	<5	<5
	Rat	37.7	21.4		
	Mouse	7.7	8.1		
9j	Human	15.7	11.2	<5	<5
	Rat	19.8	12.8		
	Mouse	6.3	7.5		

2.3. Molecular modelling

Amongst the tested analogues, compound **9i** displayed the highest inhibitory activity against FP-2. In order to further understand interactions between FP-2 and compound **9i**, docking calculations were carried out using Glide 5.7 [30,31]. Out of the four crystal structures of FP-2 reported in the Protein Databank, the structure co-crystallized with a low molecular weight, epoxysuccinate (E64) (PDB ID: 3BPF) was used. The co-crystallized inhibitor was removed from the binding pocket and to validate our docking calculations the inhibitor, E64 was redocked to FP-2. When compared with the crystal structure, the docked conformation of E64 gave rmsd of ~1.94 Å and had a Glide score of −5.48 kcal/mol (Fig. 2). Thus the crystal structure conformation was regenerated. Docked conformations of compound **9i** were ranked based on their Glide scores and the best conformation, shown in Fig. 3, gave a Glide score of −5.50 kcal/mol. In this conformation the chlorophenyl group occupied the S2 subsite whilst the trimethoxyphenyl group was in the S1 subsite. The thiazolidine-2,4-dione

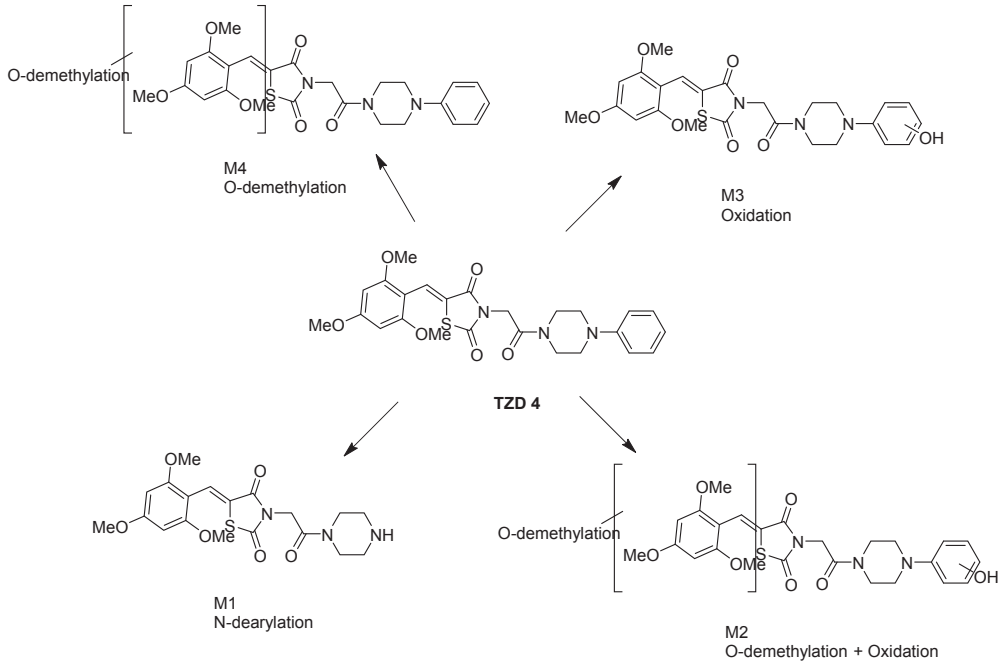

Fig. 4. Proposed microsomal metabolites of **TZD 4**.

(TZD) scaffold was placed in a position close to the active site of the enzyme but at a distance that prevents covalent bond formation with Cys42 (Fig. 3A). The docked conformation of **9i** was stabilised by hydrophobic interactions between the chlorophenyl group and hydrophobic residues Ile85, Gly83, Leu84, and Ala175 in S2 (green circles in Fig. 3B) and additionally, there are dipole–dipole interactions between His174 ND1 and atom O1 in compound **9i**, which are ~4.23 Å apart (Fig. 3B). Occupation of the S2 subsite, a site also occupied by E64, is important for specificity of cysteine proteases [32]. Therefore, the inhibitory activity of **9i** against FP-2 may be attributed to its conformation and interaction with residues like His174 that are important for enzyme inhibition activity.

2.4. Microsomal stability and metabolite identification studies

The selected analogues **TZD 4**, **9g**, **9h**, **9i** and **9j** were evaluated for their *in vitro* microsomal metabolic stability using human, rat and mouse liver microsomes as a preliminary indication of the likely *in vivo* metabolic clearance. All the compounds showed poor metabolic stability across the three species as indicated in Table 3. Metabolite identification studies were therefore carried out in order to understand the sites of metabolism contributing to this rapid clearance. The metabolism of **TZD 4** proceeds mainly by hydroxylation on the unsubstituted phenyl ring. This metabolite accounts for about 50% of the metabolism. *O*-Dealkylation, *N*-dearylation and a combination of hydroxylation and *O*-dealkylation were also detected as metabolites. Substitution on the phenyl ring, as in **9j**, shifts the metabolic hotspot to the other side of the molecule with *O*-dealkylation being the major metabolite (>50%) (Fig. 4).

2.5. Cytotoxicity studies

The *in vitro* cytotoxicity of the most active compounds **TZD 4** and **9i** was evaluated against a mammalian cell-line, Chinese Hamster Ovarian (CHO) using the 3-(4,5-dimethylthiazol-2-yl)-2,5-diphenyltetrazoliumbromide (MTT) assay. No significantly cytotoxicity was observed for **TZD 4** (IC_{50} 53.7 μM; SI = 30.5) or **9i** (IC_{50} > 188.3 μM; SI = 131.6).

3. Conclusions

Analogues of substituted thiazolidine-2,4-diones based on a hit identified from virtual screening of the commercial ZINC database for falcipain-2 inhibition were synthesized using relatively facile synthetic routes. The *in vitro* biological evaluation of these compounds against FP-2 and *P. falciparum* revealed several that had IC_{50} values in the low micromolar range. In particular, the presence of a trimethoxy-substituted phenyl ring attached to C-5 of the core 2,4-thiazolidinedione was found to be necessary for antiplasmodial activity while at position 3, a phenyl substituted piperazine ring was necessary for optimal activity. Modifications to the hit scaffold and *in silico* docking studies on falcipain-2 helped to delineate the tentative SAR of these compounds and provide insight into the requirements for activity.

Despite their notable plasmodial growth inhibition, selected compounds from this series were found to be metabolically unstable and prone to rapid degradation in human, rat and mouse hepatic microsomes *in vitro*. Metabolite identification studies revealed that metabolism occurred at the terminal phenyl substituents on both ends of the molecules, mostly through ring hydroxylation or *O*-dealkylation.

Based on these data, the thiazolidinedione class of compounds appears to be a promising novel chemotype for anti-malarial drug discovery. Since demonstrating *in vivo* efficacy in an appropriate mouse model is a prerequisite before a lead optimization campaign may be undertaken, addressing poor microsomal metabolic stability remains the priority before additional SAR explorations to improve antiplasmodial potency and other desirable properties can be undertaken.

4. Experimental section

4.1. Chemistry

4.1.1. General

^{1}H NMR spectra were recorded on a Varian Mercury Spectrometer at 300 MHz or a Varian Unity Spectrometer at 400 MHz

with Me_4Si as internal standard. ^{13}C NMR spectra were recorded at 75 and 100 MHz on a Varian Mercury Spectrometer or at 100 MHz on Varian Unity Spectrometer with Me_4Si as internal standard. High resolution mass spectra were recorded on a VG70 SEQ micromass spectrometer. Melting points were determined using a Reichert-Jung Thermovar hot-stage microscope and are uncorrected. Analytical thin-layer chromatography (TLC) was performed on aluminium-backed silica-gel 60 F_{254} (70–230 mesh) plates. Column chromatography was performed with Merck silica-gel 60 (70–230 mesh).

4.1.2. Synthesis of 2,4 thiazolidinedione derivatives

*4.1.2.1. 1-(Chloroacetyl)-phenyl piperazine (**2**).* To a solution of phenyl piperazine (2.0 g, 0.0123 mol) in DCM (60 ml), TEA (2.2 ml, 1 equiv) was added at RT and cooled the reaction mass to 0 °C. Chloroacetyl chloride (1.2 g, 1 equiv) was added drop wise at 0 °C and stirred for 1 h at RT. The saturated $NaHCO_3$ solution (60 ml) was added and stirred for 15 min at RT. The organic layer was separated and washed with brine, dried over $MgSO_4$, filtered and concentrated. The concentrated mass was purified by silica gel CC using 25–30% EtOAc–hexane to give 1-(chloroacetyl)-phenyl piperazine (1.6 g, 55%) **2** as off white solid. R_f 0.63 (30% EtOAc–hexane); Mpt. 77 °C; ^1H NMR (400 MHz, $CDCl_3$) δ: 7.30–7.25 (2H, m), 6.94–6.92 (3H, m), 4.11 (2H, s), 3.80–3.77 (4H, m), 3.70–3.67 (4H, m); ^{13}C NMR (100 MHz, $CDCl_3$) δ: 165.1, 150.8, 130.8 (2C), 120.7, 116.8 (2C), 49.7, 49.3, 46.2, 40.7, 38.7.

*4.1.2.2. 3-(2-Oxo-2-(4-phenylpiperazin-1-yl)ethyl)thiazolidine-2,4-dione (**3**).* The mixture of **2** (1.0 g, 0.418 mmol), TZDs (0.981 g, 2 equiv) and K_2CO_3 (1.15 g, 2 equiv) in acetone (130 ml) was stirred for 24 h at 60–70 °C under N_2. The reaction mass was filtered and concentrated to yellowish mass. The crude mass was purified on silica gel CC at 30–40% EtOAc:hexane afforded 3-(2-oxo-2-(4-phenylpiperazin-1-yl)ethyl)thiazolidine-2,4-dione (700 mg, 52%) **3** as white solid. R_f 0.50 (30–40% EtOAc–hexane); Mpt. 175 °C; ^1H NMR (400 MHz, $CDCl_3$) δ: 7.07–7.02 (2H, m), 6.7–6.67 (3H, m), 4.20 (2H, s), 3.8 (2H, s), 3.35–3.36 (4H, m), 3.0–2.92 (4H, m); ^{13}C NMR (100 MHz, $CDCl_3$) δ: 171.5, 171.1, 162.8, 150.7, 129.3 (2C), 126.9 (2C), 116.9, 49.5, 49.3, 44.7, 42.3 (2C), 33.9; EIMS *m/z*: 319.1; HPLC (% purity): 99%, $t_{r'} = 5.76$.

*4.1.3. General procedure for the synthesis of **TZD 4**, **4a–t***

The intermediate **3** (1 equiv), substituted benzaldehydes (1 equiv) and ammonium acetate (2 equiv) in toluene (4 ml) were irradiated on microwave at 125 °C, 220 W for 20 min. The solvent was evaporated on vacuo and crude mixture was purified on silica gel CC yielded compounds **4**, **4a–t**.

*4.1.3.1. 3-[2-Oxo-2-(4-phenylpiperazin-1-yl)ethyl]-5-(2,4,6-trimethoxybenzylidene) 1,3-thiazolidine-2,4-dione (**TZD 4**).* (50 mg, 64%) yellow solid; Mpt. 220 °C; R_f 0.56 (60% EtOAc–hexane); ^1H NMR (400 MHz, $CDCl_3$) δ: 8.23 (1H, s), 7.29–7.25 (2H, m), 6.95–6.92 (3H, m), 6.10 (2H, s), 4.55 (2H, s), 3.87 (3H, s), 3.86 (3H, s), 3.85 (3H, s), 3.78–3.67 (4H, m), 3.27–3.18 (4H, m); ^{13}C NMR (100 MHz, $CDCl_3$) δ: 167, 164.3 (2C), 163.5, 160.1 (2C), 150.8, 129.2, 128.6 (2C), 120.7, 120.2, 116.8 (2C), 104, 90.4 (2C), 55.5 (2C), 55.4, 49.5, 49.3, 44.8, 42.2, 41.8; EIMS *m/z*: 497.16; HPLC (% purity): 97.2%, $t_{r'} = 8.41$.

*4.1.3.2. 3-[2-Oxo-2-(4-phenylpiperazin-1-yl)ethyl]-5-(2,4-dimethoxybenzylidene)1,3-thiazolidine-2,4-dione (**4a**).* (38 mg, 52%) yellow solid; Mpt. 198 °C; R_f 0.60 (40% EtOAc–hexane); ^1H NMR (400 MHz, $CDCl_3$) δ: 8.18 (1H, s), 7.33 (1H, d), 7.25–7.19 (2H, m), 6.88–6.83 (3H, m), 6.52 (1H, dd, J = 2.3, 8.7 Hz), 6.40 (1H, d, J = 2.2 Hz), 4.51 (2H, s, H), 3.80 (3H, s), 3.79 (3H, s), 3.73–3.61 (4H, m), 3.21–3.12 (4H, m); ^{13}C NMR (100 MHz, $CDCl_3$) δ: 168.6, 166.3, 163.4, 163.2, 160.2, 150.8, 131, 130.1, 129.2 (2C), 120.7, 118.1, 116.8, 115.6 (2C), 105.5, 98.6, 55.5 (2C), 49.5, 49.3, 44.8, 42.2, 42.1; EIMS *m/z*: 467.09; HPLC (% purity): 99%, $t_{r'} = 8.32$.

*4.1.3.3. 3-[2-Oxo-2-(4-phenylpiperazin-1-yl)ethyl]-5-(3-methoxybenzylidene)1,3-thiazolidine-2,4-dione (**4b**).* (42 mg, 61%) yellow solid; Mpt. 189 °C; R_f 0.38 (35% EtOAc–hexane); ^1H NMR (400 MHz, $CDCl_3$) δ: 7.9 (1H, s), 7.38 (1H, t, J = 7.3 Hz), 7.32–7.25 (2H, m), 7.11 (1H, d, J = 8.3 Hz), 6.95–6.92 (5H, m), 4.59 (2H, s), 3.96 (3H, s), 3.80–3.67 (4H, m), 3.28–3.19 (4H, m); ^{13}C NMR (100 MHz, $CDCl_3$) δ: 167.8, 165.9, 162.9, 160, 150.7, 134.5, 134.4, 130.2, 129.3 (2C), 122.7, 121.8, 120.9, 116.9 (2C), 116.6, 115, 55.4, 49.6, 49.4, 44.8, 42.3 (2C); EIMS *m/z*: 437.14; HPLC (% purity): 98.2%, $t_{r'} = 7.65$.

*4.1.3.4. 3-[2-Oxo-2-(4-phenylpiperazin-1-yl)ethyl]-5-(4-methoxybenzylidene)1,3-thiazolidine-2,4-dione (**4c**).* (46 mg, 42%) yellow solid; Mpt. 238 °C; R_f 0.60 (35% EtOAc–hexane); ^1H NMR (400 MHz, $CDCl_3$) δ: 7.81 (1H, s), 7.41 (2H, d, J = 8.6 Hz), 7.24–7.18 (2H, m), 6.92 (2H, d, J = 8.8 Hz), 6.89–6.84 (3H, m), 4.51 (2H, s), 3.79 (3H, s), 3.73–3.60 (4H, m), 3.22–3.13 (4H, m); ^{13}C NMR (100 MHz, $CDCl_3$) δ: 168, 166.2, 163, 161.5, 150.6, 134.3, 132.2, 129.3 (2C), 125.9 (2C), 121.1, 120.9, 118.4, 116.9 (2C), 114.8, 55.4, 49.6, 49.4, 44.8, 42.2 (2C); EIMS *m/z*: 437.14; HPLC (% purity): 98.2%, $t_{r'} = 8.70$.

*4.1.3.5. 3-[2-Oxo-2-(4-phenylpiperazin-1-yl)ethyl]-5-(4-fluorobenzylidene)1,3-thiazolidine-2,4-dione (**4d**).* (37 mg, 56%) white solid; Mpt. 215 °C; R_f 0.62 (35% EtOAc–hexane); ^1H NMR (400 MHz, $CDCl_3$) δ: 7.83 (1H, s), 7.47 (2H, dd, J = 2.1, 5.2 Hz), 7.26–7.21 (2H, m), 7.14–7.08 (2H, m), 6.91–6.85 (3H, m), 4.53 (2H, s), 3.75–3.61 (4H, m), 3.23–3.12 (4H, m); ^{13}C NMR (100 MHz, $CDCl_3$) δ: 167.6, 165.9, 165, 162.9, 162.4, 150.5, 133.1, 132.3, 132.2, 129.5 (2C), 129.3, 121.1, 117, 116.8, 116.6, 116.4, 49.7, 49.4, 44.7, 42.3, 42.2; EIMS *m/z*: 425.1; HPLC (% purity): 95.1%, $t_{r'} = 8.35$.

*4.1.3.6. 3-[2-Oxo-2-(4-phenylpiperazin-1-yl)ethyl]-5-(4-trifluoromethoxybenzylidene) 1,3-thiazolidine-2,4-dione (**4e**).* (34 mg, 44%) yellow solid; Mpt. 190 °C; R_f 0.64 (35% EtOAc–hexane); ^1H NMR (400 MHz, $CDCl_3$) δ: 7.80 (1H, s), 7.55 (2H, dd, J = 2.1, 6.8 Hz), 7.32–7.28 (4H, m), 6.99–6.93 (3H, m), 4.60 (2H, s), 3.82–3.68 (4H, m), 3.30–3.20 (4H, m); ^{13}C NMR (100 MHz, $CDCl_3$) δ: 167.3, 165.8, 162.8, 154.6, 150.3, 132.5, 131.7 (2C), 129.3 (3C), 122.4 (2C), 121.3, 117.1 (4C), 49.8, 49.6, 44.7, 42.4, 42.2; EIMS *m/z*: 491.05; HPLC (% purity): 98.3%, $t_{r'} = 9.20$.

*4.1.3.7. 3-[2-Oxo-2-(4-phenylpiperazin-1-yl)ethyl]-5-(4-trifluoromethylbenzylidene) 1,3-thiazolidine-2,4-dione (**4f**).* (40 mg, 33%) yellow solid; Mpt. 202 °C; R_f 0.58 (40% EtOAc–hexane); ^1H NMR (400 MHz, $CDCl_3$) δ: 7.86 (1H, s), 7.66 (2H, d, J = 8.2 Hz), 7.55 (2H, d, J = 8.1 Hz), 7.26–7.21 (2H, m), 6.88–6.84 (3H, m), 4.53 (2H, s), 3.73–3.60 (4H, m), 3.21–3.12 (4H, m); ^{13}C NMR (100 MHz, $CDCl_3$) δ: 167.1, 165.6, 162.7, 150.7, 136.6, 132.2, 130.1 (3C), 129.3 (3C), 126.1 (2C), 124.3, 120.9, 116.9 (2C), 49.5, 49.3, 44.8, 42.5, 42.3; EIMS *m/z*: 475.05; HPLC (% purity): 93.5%, $t_{r'} = 9.05$.

*4.1.3.8. 3-[2-Oxo-2-(4-phenylpiperazin-1-yl)ethyl]-5-(2-chlorobenzylidene)1,3-thiazolidine-2,4-dione (**4g**).* (30 mg, 44%) white solid; Mpt. 166 °C; R_f 0.72 (40% EtOAc–hexane); ^1H NMR (400 MHz, $CDCl_3$) δ: 8.26 (1H, s), 7.54 (1H, dd, J = 2.3, 5.7 Hz), 7.47 (1H, dd, J = 2.3, 5.4 Hz), 7.38–7.35 (2H, m), 7.32–7.25 (2H, m), 6.98–6.92 (3H, m), 4.6 (2H), 3.82–3.68 (4H, m), 3.30–3.20 (4H, m); ^{13}C NMR (100 MHz, $CDCl_3$) δ: 167.6, 165.4, 162.9, 150.3, 136, 131.8, 131.3, 130.6, 130.4, 129.3 (2C), 128.9, 127.2, 124.5, 121.1, 116.9 (2C), 49.7, 49.5, 44.7, 42.3, 42.2; EIMS *m/z*: 440.99; HPLC (% purity): 99%, $t_{r'} = 7.83$.

*4.1.3.9. 3-[2-Oxo-2-(4-phenylpiperazin-1-yl)ethyl]-5-(2-bromobenzylidene)1,3-thiazolidine-2,4-dione (**4h**).* (28 mg, 37%) white solid; Mpt. 138 °C; R_f 0.68 (40% EtOAc–hexane); ^{1}H NMR (400 MHz, $CDCl_3$) δ: 8.14 (1H, s), 7.62 (1H, d, J = 7.9 Hz), 7.47 (1H, d, J = 7.8 Hz), 7.35 (1H, t, J = 7.3 Hz), 7.26–7.19 (3H, m), 6.89–6.84 (3H, m), 4.53 (2H, s), 3.72–3.60 (4H, m), 3.21–3.13 (4H, m); ^{13}C NMR (100 MHz, $CDCl_3$) δ: 167.6, 165.3, 162.8, 150.7, 133.7, 133.6, 133.2, 131.5, 129.3 (2C), 129, 127.9, 126.2, 124.6, 120.8, 116.9 (2C), 49.5, 49.3, 44.8, 42.3 (2C); EIMS m/z: 485.06; HPLC (% purity): 98%, $t_{r'}$ = 9.03.

*4.1.3.10. 3-[2-Oxo-2-(4-phenylpiperazin-1-yl)ethyl]-5-(3-isopropylbenzylidene)1,3-thiazolidine-2,4-dione (**4i**).* (36 mg, 32%) white solid; Mpt. 170 °C; R_f 0.54 (30% EtOAc–hexane); ^{1}H NMR (400 MHz, $CDCl_3$) δ: 7.86 (1H, s), 7.34 (1H, d, J = 7.6 Hz), 7.30 (1H, d, J = 1.8 Hz), 7.29–7.19 (4H, m), 6.89–6.84 (3H, m), 4.52 (2H, s), 3.73–3.60 (4H, m), 3.21–3.11 (4H, m), 2.89 (1H, sep, J = 6.9 Hz), 1.21 (6H, m); ^{13}C NMR (100 MHz, $CDCl_3$) δ: 168, 166, 163, 150, 149.9, 134.8, 133, 129.3 (2C), 129.2, 129, 128.3, 127.7, 121.1, 120.9, 116.9 (2C), 49.6, 49.4, 44.8, 42 (2C), 34, 23.8 (2C); EIMS m/z: 449.14; HPLC (% purity): 96.4%, $t_{r'}$ = 9.96.

*4.1.3.11. 3-[2-Oxo-2-(4-phenylpiperazin-1-yl)ethyl]-5-(2,5-ditrifluoromethylbenzylidene) 1,3-thiazolidine-2,4-dione (**4j**).* (42 mg, 30%) yellow solid; Mpt. 156 °C; R_f 0.72 (25% EtOAc–hexane); ^{1}H NMR (400 MHz, $CDCl_3$) δ: 8.07 (1H, s), 7.85–7.83 (2H, m), 7.71 (1H, d, J = 8.7 Hz), 7.25–7.21 (2H, m), 6.89–6.85 (3H, m), 4.53 (2H, s), 3.74–3.60 (4H, m), 3.22–3.13 (4H, m); ^{13}C NMR (100 MHz, $CDCl_3$) δ: 166.4, 164.4, 162.6, 150.6, 134.5, 133.4, 129.3 (2C), 128.4, 128.1, 127.6 (2C), 127.5, 126.5 (2C), 125.9, 121, 116.9 (2C), 49.6, 49.4, 44.8, 42.5, 42.3; EIMS m/z: 543.06; HPLC (% purity): 98%, $t_{r'}$ = 9.4.

*4.1.3.12. 3-[2-Oxo-2-(4-phenylpiperazin-1-yl)ethyl]-5-(2-trifluoromethoxybenzylidene) 1,3-thiazolidine-2,4-dione (**4k**).* (32 mg, 27%) yellow solid; Mpt. 167 °C; R_f 0.52 (35% EtOAc–hexane); ^{1}H NMR (400 MHz, $CDCl_3$) δ: 8.07 (1H, s), 7.54 (1H, dd, J = 1.8, 7.5 Hz), 7.41 (1H, dd, J = 1.8, 7.8 Hz), 7.36 (1H, dd, J = 1.5, 7.5 Hz), 7.26–7.19 (2H, m), 6.89–6.84 (4H, m), 4.53 (2H, s), 3.73–3.60 (4H, m), 3.23–3.12 (4H, m); ^{13}C NMR (100 MHz, $CDCl_3$) δ: 167.4, 165.4, 162.8, 150.7, 148.1, 131.7, 131.4, 129.3 (2C), 129, 127.2, 127.1, 126.8, 124.7, 121.3, 120.9, 116.9 (2C), 49.6, 49.4, 44.8, 42.4, 42.3; EIMS m/z: 491.11; HPLC (% purity): 98.9%, $t_{r'}$ = 9.15.

*4.1.3.13. 3-[2-Oxo-2-(4-phenylpiperazin-1-yl)ethyl]-5-(3-trifluoromethoxybenzylidene)1,3-thiazolidine-2,4-dione (**4l**).* (40 mg, 32%) yellow solid; Mpt. 160 °C; R_f 0.64 (35% EtOAc–hexane); ^{1}H NMR (400 MHz, $CDCl_3$) δ: 7.82 (1H, s), 7.45 (1H, t, J = 7.8 Hz), 7.38 (1H, dd, J = 1.2, 6.3 Hz), 7.29–7.19 (4H, m), 6.90–6.84 (3H, m), 4.53 (2H, s), 3.74–3.60 (4H, m), 3.23–3.12 (4H, m); ^{13}C NMR (100 MHz, $CDCl_3$) δ: 167.2, 165.6, 162.7, 150.6, 149.7, 135.2, 132.3, 130.7, 129.3 (2C), 128 (2C), 123.6, 122.5, 122.2, 120.9, 116.9 (2C), 49.6, 49.4, 44.8, 42.4, 42.3; EIMS m/z: 491.10; HPLC (% purity): 99%, $t_{r'}$ = 9.19.

*4.1.3.14. 3-[2-Oxo-2-(4-phenylpiperazin-1-yl)ethyl]-5-(3-fluorobenzylidene)1,3-thiazolidine-2,4-dione (**4m**).* (42 mg, 40%) yellow solid; Mpt. 199 °C; R_f 0.58 (30% EtOAc–hexane); ^{1}H NMR (400 MHz, $CDCl_3$) δ: 7.81 (1H, s), 7.24–7.35 (1H, m), 7.26–7.19 (3H, m), 7.17–7.12 (1H, m), 7.06 (1H, dd, J = 2.5, 8.3 Hz), 6.90–6.85 (3H, m), 4.53 (2H, s), 3.74–3.60 (4H, m), 3.22–3.12 (4H, m); ^{13}C NMR (100 MHz, $CDCl_3$) δ: 167.4, 165.7, 164.2, 162.8, 150.6, 135.3, 132.8, 130.8, 130.7, 129.3, 125.8, 123.1, 121, 117.6, 117.4, 116.9, 116.7, 49.6, 49.4, 44.8, 42.4, 42.3; EIMS m/z: 425.08; HPLC (% purity): 98.9%, $t_{r'}$ = 8.19.

*4.1.3.15. 3-[2-Oxo-2-(4-phenylpiperazin-1-yl)ethyl]-5-(3,4-difluorobenzylidene)1,3-thiazolidine-2,4-dione (**4n**).* (50 mg, 45%) yellow solid; Mpt. 188 °C; R_f 0.74 (30% EtOAc–hexane); ^{1}H NMR (400 MHz, $CDCl_3$): δ 7.74 (1H, s), 7.28 (1H, dd, J = 1.8, 8.2 Hz), 7.24 (1H, d, J = 2.1 Hz), 7.23–7.18 (3H, m), 6.89–6.85 (3H, m), 4.52 (2H, s), 3.73–3.59 (4H, m), 3.22–3.12 (4H, m); ^{13}C NMR (100 MHz, $CDCl_3$) δ: 167.1, 165.6, 162.7, 150.6, 131.8, 130.4, 129.3 (2C), 126.8, 122.7, 121, 118.8, 118.6, 118.4, 118.2, 116.9 (2C), 49.6, 49.4, 44.8, 42.4, 42.3; EIMS m/z: 443.04; HPLC (% purity): 95.6%, $t_{r'}$ = 8.57.

*4.1.3.16. 3-[2-Oxo-2-(4-phenylpiperazin-1-yl)ethyl]-5-(4-chlorobenzylidene)1,3-thiazolidine-2,4-dione (**4o**).* (43 mg, 39%) light yellow solid; Mpt. 240 °C; R_f 0.64 (35% EtOAc–hexane); ^{1}H NMR (400 MHz, DMSO) δ: 7.96 (1H, s), 7.67 (2H, d, J = 8.6 Hz), 7.60 (2H, d, J = 8.7 Hz), 7.25–7.20 (2H, m), 6.96 (2H, d, J = 7.8 Hz), 6.79 (1H, t, J = 7.2 Hz), 4.66 (2H, s), 3.69–3.57 (4H, m), 3.22–3.10 (4H, m); ^{13}C NMR (100 MHz, $CDCl_3$) δ: 167.4, 165.8, 162.8, 150.2, 136.7, 132.9, 131.7, 131.3, 129.5 (2C), 129.3 (2C), 122.1, 121.1, 120, 117 (2C), 49.7, 49.4, 44.7, 42.4, 42.2; EIMS m/z: 441.02; HPLC (% purity): 99%, $t_{r'}$ = 9.31.

*4.1.3.17. 3-[2-Oxo-2-(4-phenylpiperazin-1-yl)ethyl]-5-(2,4-dichlorobenzylidene)1,3-thiazolidine-2,4-dione (**4p**).* (50 mg, 42%) yellow solid; Mpt. 223 °C; R_f 0.60 (35% EtOAc–hexane); ^{1}H NMR (400 MHz, $CDCl_3$) δ: 8.11 (1H, s), 7.44 (1H, d, J = 2.0 Hz), 7.41 (1H, d, J = 8.2 Hz), 7.28 (1H, dd, J = 2.0, 8.4 Hz), 7.25–7.19 (2H, m), 6.88–6.83 (3H, m), 4.53 (2H, s), 3.74–3.60 (4H, m), 3.22–3.12 (4H, m); ^{13}C NMR (100 MHz, $CDCl_3$) δ: 167.1, 165.3, 162.7, 150.6, 136.8, 136.6, 130.4 (2C), 130.3, 129.6, 129.3 (2C), 127.7, 124.9, 121, 116.9 (2C), 49.6, 49.4, 44.8, 42.4, 42.3; EIMS m/z: 475.04; HPLC (% purity): 99%, $t_{r'}$ = 9.55.

*4.1.3.18. 3-[2-Oxo-2-(4-phenylpiperazin-1-yl)ethyl]-5-(3-carboxybenzylidene)1,3-thiazolidine-2,4-dione (**4q**).* (46 mg, 41%) white solid; Mpt. 214 °C; R_f 0.48 (15% MeOH–DCM); ^{1}H NMR (400 MHz, DMSO) δ: 8.21 (1H, s), 8.04 (1H, d, J = 7.5 Hz), 7.98 (1H, s), 7.71 (1H, d, J = 7.0 Hz), 7.54 (1H, t, J = 7.7 Hz), 7.24–7.20 (2H, m), 6.98–6.79 (3H, m), 4.66 (2H, s), 3.68–3.58 (4H, m), 3.22–3.10 (4H, m); ^{13}C NMR (100 MHz, DMSO) δ: 169.6, 167.5, 165.7, 163.7, 151.1, 138, 133.9, 132.3, 131.9, 130.8 (2C), 129.4 (2C), 121.5, 119.9 (2C), 116.4 (2C), 49, 48.6, 44.4, 43.1, 42; EIMS m/z: 451.05; HPLC (% purity): 99%, $t_{r'}$ = 6.89.

*4.1.3.19. 3-[2-Oxo-2-(4-phenylpiperazin-1-yl)ethyl]-5-(4-methylbenzylidene)1,3-thiazolidine-2,4-dione (**4r**).* (48 mg, 45%) yellow solid; Mpt. 239 °C; R_f 0.64 (35% EtOAc–hexane); ^{1}H NMR (400 MHz, $CDCl_3$) δ: 7.84 (1H, s), 7.35 (2H, d, J = 8.1 Hz), 7.26–7.19 (4H, m), 6.90–6.84 (3H, m), 4.53 (2H, s), 3.72–3.60 (4H, m), 3.21–3.12 (4H, m), 2.34 (3H, s); ^{13}C NMR (100 MHz, $CDCl_3$) δ: 168, 166.1, 163, 150.7, 141.3, 134.5, 130.5, 130.3, 130.1, 130, 129.4, 129.3 (2C), 120.9, 120.2, 116.9, 116.8, 49.6, 49.4, 44.8, 42.2 (2C), 21.5; EIMS m/z: 421.13; HPLC (% purity): 98.9%, $t_{r'}$ = 9.05.

*4.1.3.20. 3-[2-Oxo-2-(4-phenylpiperazin-1-yl)ethyl]-5-(3-methylbenzylidene)1,3-thiazolidine-2,4-dione (**4s**).* (38 mg, 36%) yellow solid; Mpt. 194 °C; R_f 0.66 (35% EtOAc–hexane); ^{1}H NMR (400 MHz, $CDCl_3$) δ: 7.84 (1H, s), 7.32 (1H, d, J = 8.2 Hz), 7.28–7.25 (3H, m), 7.23 (1H, d, J = 1.2 Hz), 7.21–7.17 (1H, m), 6.95–6.92 (3H, m), 4.53 (2H, s), 3.74–3.62 (4H, m), 3.21–3.12 (4H, m), 2.34 (3H, s); ^{13}C NMR (100 MHz, $CDCl_3$) δ: 168, 166, 163, 150.7, 139, 134.6, 133.2, 131.4, 130.9, 129.3 (2C), 129.1, 127.3, 120.9, 120.2, 116.9 (2C), 49.6, 49.4, 44.8, 42.3 (2C), 21.3; EIMS m/z: 421.14; HPLC (% purity): 99.2%, $t_{r'}$ = 7.50.

*4.1.3.21. 3-[2-Oxo-2-(4-phenylpiperazin-1-yl)ethyl]-5-benzylidene-1,3-thiazolidine-2,4-dione (**4t**).* (38 mg, 60%) white solid; Mpt. 211 °C; R_f 0.70 (25% EtOAc–hexane); ^{1}H NMR (400 MHz, DMSO) δ: 7.86 (1H, s), 7.46–7.36 (5H, m), 7.24–7.18 (2H, m), 6.89–6.84 (3H, m), 4.52 (2H, s), 3.73–3.60 (4H, m), 3.22–3.12 (4H, m); ^{13}C NMR (100 MHz, DMSO) δ: 167.9, 166, 162.9, 150.6, 134.4, 133.2, 130.5 (2C), 130.2 (2C), 129.3, 129.2 (2C), 121.4, 120.9, 117, 116.9, 49.6, 49.2, 44.8, 42.3 (2C); EIMS *m*/*z*: 407.10; HPLC (% purity): 99%, $t_{r'}$ = 8.58.

*4.1.3.22. 2-(2,4-Dioxo-1,3-thiazolidin-3-yl)acetic acid (**7**).* To a solution of TZD (1 g, 8.53 mmol) in dry DMF (5 ml), NaH (340 mg, 1 equiv) was added and stirred for 10 min at room temperature. The bromoacetic ester (786 mg, 1 equiv) was added drop wise in the reaction mass and stirred for 24 h at room temperature. The reaction mass was extracted with H_2O (20 ml) and DCM (20 ml). The organic layer was washed with 5% HCl solution, dried over $MgSO_4$, concentrated and purified on silica gel CC using 50% ethylacetate–hexane afforded methyl 2-(2,4-dioxo-1,3-thiazolidin-3-yl) acetate (1.4 g, 87%) (**8**) as yellow liquid. R_f 0.46 (50% EtOAc–hexane); ^{1}H NMR (400 MHz, $CDCl_3$) δ: 4.27 (2H, s, $-N\underline{CH_2}COOCH_3$), 3.97 (2H, s, H5), 3.69 (3H, s, $-NCH_2COO\underline{CH_3}$); ^{13}C NMR (100 MHz, DMSO) δ: 170.9, 170.5, 166.6, 52.8, 41.9, 33.8; EIMS *m*/*z*: 189.03. The yellow liquid was refluxed with 40% HBr(10 ml) for 4 h at 110 °C. Water (10 ml) was added and reaction mass was extracted with ethylacetate (50 ml × 3). The combined organic layer was dried over $MgSO_4$ filtered and concentrated on vacuo gave 2-(2,4-dioxo-1,3-thiazolidin-3-yl)acetic acid (2.1 g, 52%) (**7**) as pale white solid. R_f 0.22 (EtOAc); Mpt. 143 °C; ^{1}H NMR (400 MHz, DMSO) δ: 4.34 (2H, s), 3.84 (2H, s); ^{13}C NMR (100 MHz, DMSO) δ: 171.5, 168.5, 168.1, 41.4, 33.2; EIMS *m*/*z*: 175.

*4.1.3.23. 2-(5-(2,4,6-Trimethoxybenzylidene)-2,4-dioxo-thiazolidin-3-yl) acetic acid (**8**).* To a solution of **7** (1 equiv) in absolute ethanol (10 ml), 2,4,6-trimethoxybenzaldehyde (1.1 equiv), piperidine (0.6 ml) and AcOH (2–4 drops) was added and reaction mass was stirred for 5 h at 40–50 °C. The reaction solvent was evaporated and water(40 ml) was added. The aqueous layer was extracted with ethylacetate (50 ml × 2) and then pH of aqueous layer was acidified to 3 pH using 5% HCl solution. The acidified aqueous layer was extracted with ethylacetate (50 ml × 3). The combined organic layer was dried over $MgSO_4$ filtered, concentrated followed by silica gel CC using 5–15% MeOH–DCM afforded 2-(5-(2,4,6-trimethoxybenzylidene)-2,4-dioxo-thiazolidin-3-yl) acetic acid (1.4 g, 69%) **8** as yellow solid. Mpt. 184 °C; R_f 0.48 (15% MeOH-DCM); ^{1}H NMR (400 MHz, DMSO) δ: 8.02 (1H, s), 6.30 (2H, s), 4.24 (2H, s), 3.86 (6H, s), 3.85 (3H, s); ^{13}C NMR (100 MHz, DMSO) δ: 168.6, 166.4 (2C), 165, 160.2 (2C), 127.9, 119.3, 103.5, 91.5 (2C), 56.2 (3C), 42.5; EIMS *m*/*z*: 353.06; HPLC (% purity): 98%, $t_{r'}$ = 12.44.

*4.1.4. General procedure for the synthesis of **9a**–**j***

The solution of **8** (1 equiv) and substituted phenyl piperazine (1 equiv) in dry DMF (5 ml) was cooled to 0 °C. The *N*-ethyl-*N*′-(dimethyaminopropyl)carbodimide hydrochloride (EDC·HCl) (1 equiv), 1-hyroxybenzotriazole hydrate (HOBt·H_2O) (1 equiv) and DIPEA (2 equiv) were added and the resulting mixture stirred for 24 h at room temperature. H_2O (40 ml) was added to reaction mass and extracted with ethylacetate (40 ml × 3). The combined organic layer was washed with saturated aqueous $NaHCO_3$ solution (30 ml), brine (30 ml), dried over $MgSO_4$ and concentrated to give crude mass which were purified on silica gel CC to afforded desired products **9a**–**j**.

*4.1.4.1. 3-[2-Oxo-2-(piperazin-1-yl)ethyl]-5-(2,4,6-trimethoxybenzylidene)-1,3-thiazolidine-2,4-dione (**9a**).* (30 mg, 42%) yellow solid; Mpt. 109 °C; R_f 0.42 (20% MeOH–DCM); ^{1}H NMR (400 MHz, CD_3OD) δ: 8.19 (1H, s), 6.26 (2H, s), 4.60 (2H, s), 3.89 (6H, s), 3.87 (3H, s), 3.67–3.62 (4H, m), 3.05–2.93 (4H, m); ^{13}C NMR (100 MHz, $CDCl_3$) δ: 169.7, 167.5, 166.9, 164.3, 160.2 (2C), 128.8, 119.9, 102.7, 90.4 (2C), 55.5 (2C), 55.4, 44.5 (2C), 43, 41.9, 41.8; EIMS *m*/*z*: 421.26; HPLC (% purity): 99%, $t_{r'}$ = 14,41.

*4.1.4.2. 3-[2-Oxo-2-(4-methylpiperazin-1-yl)ethyl]-5-(2,4,6-trimethoxybenzylidene)-1,3-thiazolidine-2,4-dione (**9b**).* (60 mg, 61%) white solid; Mpt. 183 °C; R_f 0.76 (5% MeOH–EtOAc); ^{1}H NMR (400 MHz, $CDCl_3$) δ: 8.14 (1H, s), 6.02 (2H, s), 4.42 (2H, s), 3.78 (6H, s), 3.77 (3H, s), 3.59–3.48 (4H, m), 2.43–2.36 (4H, m), 2.27 (3H, s); ^{13}C NMR (100 MHz, $CDCl_3$) δ: 169.8, 167, 164.3, 163.3, 160.1 (2C), 128.5, 120.2, 104.6, 90.4 (2C), 55.5 (2C), 55.4, 54.6, 54.3, 45.8, 44.5, 42, 41.8; EIMS *m*/*z*: 435.13; HPLC (% purity): 99%, $t_{r'}$ = 11.17.

*4.1.4.3. 3-[2-Oxo-2-(4-cyclohexylpiperazin-1-yl)ethyl]-5-(2,4,6-trimethoxybenzylidene)-1,3-thiazolidine-2,4-dione (**9c**).* (65 mg, 44%) light yellow solid; Mpt. 182 °C; R_f 0.72 (5% MeOH–EtOAc); ^{1}H NMR (400 MHz, $CDCl_3$) δ: 8.21 (1H, s), 6.10 (2H, s), 4.49 (2H, s), 3.86 (6H, s), 3.85 (3H, s), 3.61–3.48 (4H, m), 2.63–2.54 (4H, m), 2.30 (1H, m), 1.82–1.18 (10H, m); ^{13}C NMR (100 MHz, $CDCl_3$) δ: 169.8, 167, 164.2, 163.1, 160.1 (2C), 128.6, 120.3, 104.6, 90.4 (2C), 63.4, 55.4 (2C), 55.3, 48.9, 48.4, 45.3, 42.7, 41.9, 28.8 (2C), 26.2, 25.8 (2C); EIMS *m*/*z*: 503.12; HPLC (% purity): 99%, $t_{r'}$ = 11.84.

*4.1.4.4. 3-[2-Oxo-2-(4-pyridylpiperazin-1-yl)ethyl]-5-(2,4,6-trimethoxybenzylidene)-1,3-thiazolidine-2,4-dione (**9d**).* (65 mg, 58%) reddish solid; Mpt. 217 °C; R_f 0.38 (15% MeOH–DCM); ^{1}H NMR (400 MHz, DMSO) δ: 8.17 (2H, d, J = 6.5 Hz), 8.01 (1H, s), 6.85 (2H, d, J = 6.5 Hz), 6.31 (2H, s), 4.58 (2H, s), 3.86 (6H, s), 3.85 (3H, s), 3.70–3.54 (4H, m), 3.45–3.27 (4H, m); ^{13}C NMR (100 MHz, $CDCl_3$) δ: 169.7, 167, 164.4, 163.8, 160.2 (2C), 154.8, 148.7 (2C), 128.8, 119.8, 108.5, 108.4, 108.3, 90.4 (2C), 55.5 (2C), 55.4, 45.6 (2C), 44, 41.7, 41.3; EIMS *m*/*z*: 498.08; HPLC (% purity): 99%, $t_{r'}$ = 10.96.

*4.1.4.5. 3-[2-Oxo-2-(4-(4-methoxyphenyl)piperazin-1-yl)ethyl]-5-(2,4,6-trimethoxybenzylidene)-1,3-thiazolidine-2,4-dione (**9e**).* (50 mg, 42%) yellow solid; Mpt. 182 °C; R_f 0.56 (35% EtOAc–hexane); ^{1}H NMR (400 MHz, $CDCl_3$) δ: 8.21 (1H, s), 6.92 (2H, d, J = 8.8 Hz), 6.85 (2H, d, J = 9.0 Hz), 6.10 (2H, m), 4.55 (2H, m), 3.86 (6H, s), 3.85 (3H, s), 3.77 (3H, s), 3.78–3.66 (4H, m), 3.13–3.06 (4H, m); ^{13}C NMR (100 MHz, $CDCl_3$) δ: 169.8, 167, 164.3 (2C), 163.4, 160.1 (2C), 145.2, 128.6, 120.2, 119.1 (2C), 114.6 (2C), 104, 90.4 (2C), 55.5 (2C), 55.4, 51.1, 44.9 (2C), 42.3, 41.9 (2C); EIMS *m*/*z*: 527.09; HPLC (% purity): 99%, $t_{r'}$ = 13.47.

*4.1.4.6. 3-[2-Oxo-2-(4-phenoxypiperazin-1-yl)ethyl]-5-(2,4,6-trimethoxybenzylidene)-1,3-thiazolidine-2,4-dione (**9f**).* (62 mg, 52%) white solid; Mpt. 126 °C; R_f 0.30 (EtOAc); ^{1}H NMR (300 MHz, DMSO) δ: 8.04 (1H, s), 7.46–7.41 (5H, m), 6.31 (2H, m), 4.55 (2H, s), 3.84 (6H, s), 3.83 (3H, s), 3.60–3.49 (8H, m); ^{13}C NMR (100 MHz, $CDCl_3$) δ: 170.6, 169.7, 167, 164.4, 163.8, 160.2 (2C), 135.1, 130.1, 128.7 (2C), 128.6, 127.1 (2C), 119.9, 104.5, 90.4 (2C), 55.8 (2C), 55.4, 44.8, 41.8 (4C); EIMS *m*/*z*: 525.04; HPLC (% purity): 99%, $t_{r'}$ = 12.51.

*4.1.4.7. 3-[2-Oxo-2-(4-(2-chlorophenyl)piperazin-1-yl)ethyl]-5-(2,4,6-trimethoxybenzylidene)-1,3-thiazolidine-2,4-dione (**9g**).* (60 mg, 50%) yellow solid; Mpt. 179 °C; R_f 0.68 (50% EtOAc–hexane); ^{1}H NMR (400 MHz, $CDCl_3$) δ: 8.23 (1H, s), 7.38 (1H, d, J = 8.2 Hz), 7.22 (1H, t, J = 8.2 Hz), 7.03–6.99 (2H, m), 6.1 (2H, s), 4.55 (2H, s), 3.86 (6H, s), 3.85 (3H, s), 3.81–3.67 (4H, m), 3.12–3.03 (4H, m); ^{13}C NMR (100 MHz, $CDCl_3$) δ: 169.8, 167, 164.3, 163.6, 160.1 (2C), 151.8, 135.1, 130.2, 129.7, 128.6, 120.3, 116.5, 114.5, 104.6, 90.4 (2C), 55.6, 55.5, 55.4, 48.9, 48.8, 44.6, 42, 41.8; EIMS *m*/*z*: 531.05; HPLC (% purity): 99%, $t_{r'}$ = 14.41.

*4.1.4.8. 3-[2-Oxo-2-(4-(3-chlorophenyl)piperazin-1-yl)ethyl]-5-(2,4,6-trimethoxybenzylidene)-1,3-thiazolidine-2,4-dione (**9h**).* (55 mg, 46%) yellow solid; Mpt. 175 °C; R_f 0.70 (50% EtOAc–hexane); ^{1}H NMR (400 MHz, $CDCl_3$) δ: 8.23 (1H, s), 7.17 (1H, t, J = 8.0 Hz), 6.88 (1H, d, J = 1.4 Hz), 6.86 (1H, d, J = 7.6 Hz), 6.78 (1H, d, J = 7.6 Hz), 6.1 (2H, s), 4.54 (2H, s), 3.86 (6H, s), 3.85 (3H, s), 3.77–3.66 (4H, m), 3.26–3.20 (4H, m); ^{13}C NMR (100 MHz, $CDCl_3$) δ: 169.8, 167, 164.3, 163.5, 160.1 (2C), 148.5, 130.7, 129, 128.6, 127.7, 124.4, 120.6, 120.2, 104.6, 90.4 (2C), 55.5 (2C), 55.4, 51.3, 50.9, 45.2, 42.6, 41.9; EIMS m/z: 531.03; HPLC (% purity): 99%, $t_{r'}$ = 14.54.

*4.1.4.9. 3-[2-Oxo-2-(4-(4-chlorophenyl)piperazin-1-yl)ethyl]-5-(2,4,6-trimethoxybenzylidene)-1,3-thiazolidine-2,4-dione (**9i**).* (56 mg, 47%) yellow solid; Mpt. 187 °C; R_f 0.70 (50% EtOAc–hexane); ^{1}H NMR (400 MHz, $CDCl_3$) δ: 8.2 (1H, s), 7.20 (2H, d, J = 8.9 Hz), 6.83 (2H, d, J = 8.9 Hz), 6.07 (2H, s), 4.52 (2H, s), 3.83 (6H, s), 3.79 (3H, s), 3.76–3.64 (4H, m), 3.20–3.12 (4H, m); ^{13}C NMR (100 MHz, $CDCl_3$) δ: 169.8, 167, 164.3, 163.4, 160.1 (2C), 145.2, 128.6 (2C), 120.2, 119.1 (2C), 114.6 (2C), 104, 90.4 (2C), 55.5 (2C), 55.4, 51.1 (2C), 44.9, 42.3, 41.9; EIMS m/z: 531.01; HPLC (% purity): 99%, $t_{r'}$ = 14.38.

*4.1.4.10. 3-[2-Oxo-2-(4-(4-cyanophenyl)piperazin-1-yl)ethyl]-5-(2,4,6-trimethoxybenzylidene)-1,3-thiazolidine-2,4-dione (**9j**).* (50 mg, 48%) yellow solid; Mpt. 205 °C; R_f 0.58 (70% EtOAc–hexane); ^{1}H NMR (300 MHz, $CDCl_3$) δ: 8.14 (1H, s), 7.42 (2H, d, J = 8.9 Hz), 6.78 (2H, d, J = 8.9 Hz), 6.02 (2H, s), 4.46 (2H, s), 3.78 (9H, s), 3.74–3.62 (4H, m), 3.39–3.28 (4H, m); ^{13}C NMR (100 MHz, $CDCl_3$) δ: 169.7, 167, 164.4, 163.8, 160.2 (2C), 150.2, 133.6, 128.8, 128.7, 119.8, 119.6, 114.6, 104.5, 104.4, 101.4, 90.4, 90.3, 55.6, 55.5, 55.4, 47 (2C), 44.2, 41.8, 41.5; EIMS m/z: 522.01; HPLC (% purity): 99%, $t_{r'}$ = 13.

*4.1.4.11. 5-(2,4,6-Trimethoxybenzylidene)-1,3-thiazolidine-2,4-dione (**10**).* To a solution of TZD (1 equiv) in AcOH (4 ml), 2,4,6-trimethoxybenzaldehyde(1 equiv) and NH_4OAc (2 equiv) was added and reaction mass was stirred for 16–24 h at 110–115 °C. Filter the reaction mass and washed with EtOH and hexane. The crude mass was dried in oven at 80–100 °C afforded **10** as yellow solid(580 mg, 76%) yellow solid; Mpt. 271 °C; R_f 0.48 (50% EtOAc–hexane); ^{1}H NMR (400 MHz, DMSO) δ: 7.85 (1H, s), 6.28 (2H, s), 3.83 (9H, s); ^{13}C NMR (100 MHz, DMSO) δ: 169.7, 168.7, 164.6, 160 (2C), 126.2, 122.2, 103.6, 91.5 (2C), 56.1 (3C); EIMS m/z: 295.01; HPLC (% purity): 99% $t_{r'}$ = 12.32.

*4.1.5. General procedure for the synthesis of **11a–i***

To a solution of **10** (1 equiv) in dry DMF (5 ml), NaH (1 equiv) was added and stirred for 10 min at room temperature. The alkyl/substituted aryl halide (1 equiv) was added in the reaction mass and stirred for 14 h at room temperature. The reaction mass was extracted with H_2O (20 ml) and ethylacetate (20 ml). The organic layer was washed with 5% HCl solution, dried over $MgSO_4$, concentrated and purified on Si gel CC using binary solution of ethyl acetate: hexane at different polarities afforded compounds **11a–i** as yellow solids.

*4.1.5.1. 3-Methyl-5-(E/Z)(2,4,6-trimethoxybenzylidene)-1,3-thiazolidine-2,4-dione (**11a**).* (60 mg, 72%) yellow solid; Mpt. 180 °C; R_f 0.58 (50% EtOAc–hexane); ^{1}H NMR (400 MHz, $CDCl_3$) δ: 8.13 (1H, s), 6.03 (2H, s), 3.79 (6H, s), 3.78 (3H, s), 3.12 (3H, s); ^{13}C NMR (100 MHz, $CDCl_3$) δ: 169.9, 167.5, 164.2, 160.9 (2C), 127.9, 122.4, 104.5, 90.4 (2C), 55.5 (2C), 55.4, 29.6; EIMS m/z: 309.06; HPLC (% purity): 99%, $t_{r'}$ = 13.24.

*4.1.5.2. 3-Ethyl-5-(E/Z)(2,4,6-trimethoxybenzylidene)-1,3-thiazolidine-2,4-dione (**11b**).* (58 mg, 66%) yellow solid; Mpt. 123 °C; R_f 0.60 (50% EtOAc–hexane); ^{1}H NMR (400 MHz, $CDCl_3$) δ: 8.12 (1H, s), 6.02 (2H, s), 3.79 (6H, s), 3.78 (3H, s), 3.68 (2H, q, J = 7.0 Hz), 1.18 (3H, t, J = 7.0 Hz); ^{13}C NMR (100 MHz, $CDCl_3$) δ: 169.6, 167.7, 164.1, 160 (2C), 127.7, 120.4, 104.6, 90.1 (2C), 55.4 (3C), 36.5, 13.1; EIMS m/z: 323.08; HPLC (% purity): 99%, $t_{r'}$ = 13.88.

*4.1.5.3. 3-Benzyl-5-(E/Z)(2,4,6-trimethoxybenzylidene)-1,3-thiazolidine-2,4-dione (**11c**).* (56 mg, 54%) yellow solid; Mpt. 164 °C; R_f 0.62 (50% EtOAc–hexane); ^{1}H NMR (400 MHz, $CDCl_3$) δ: 8.14 (1H, s), 7.36 (2H, d, J = 7.6 Hz), 7.26–7.19 (3H, m), 6.02 (2H, m), 4.79 (2H, m), 3.78 (6H, s), 3.77 (3H, s); ^{13}C NMR (100 MHz, $CDCl_3$) δ: 170.6, 167.1, 164.1, 160.2 (2C), 135.7, 128.8, 128.5, 128.1, 128, 127.9 (2C), 120.2, 104.5, 90.1 (2C), 55.5 (2C), 55.4, 44.8; EIMS m/z: 385.1; HPLC (% purity): 99%, $t_{r'}$ = 15.92.

*4.1.5.4. 3-(4-Methylbenzyl)-5-(E/Z)(2,4,6-trimethoxybenzylidene)-1,3-thiazolidine-2,4-dione (**11d**).* (70 mg, 64.8%) yellow solid; Mpt. 167 °C, R_f 0.68 (35% EtOAc–hexane); ^{1}H NMR (400 MHz, $CDCl_3$) δ: 8.14 (1H, s), 7.27 (2H, d, J = 7.9 Hz), 6.92 (2H, d, J = 7.7 Hz), 6.03 (2H, m), 4.76 (2H, m), 3.79 (9H, s), 2.25 (3H, s); ^{13}C NMR (100 MHz, $CDCl_3$) δ: 167.1, 164.2, 160 (3C), 137.6, 132.8, 129.2, 129.1, 128.9, 128.8, 128, 120.4, 104.6, 90.4 (2C), 55.5, 55.4 (2C), 44.5, 21.1; EIMS m/z: 399.09; HPLC (% purity): 99%, $t_{r'}$ = 15.65.

*4.1.5.5. 3-(2,4-Difluorobenzyl)-5-(2,4,6-trimethoxybenzylidene)-1,3-thiazolidine-2,4-dione (**11e**).* (50 mg, 43%) yellow solid; Mpt. 147 °C; R_f 0.62 (30% EtOAc–hexane); ^{1}H NMR (400 MHz, $CDCl_3$) δ: 8.17 (1H, s), 7.30 (1H, d, J = 8.1 Hz), 6.78 (1H, dd, J = 2.6, 8.6 Hz), 6.73 (1H, d, J = 2.5 Hz), 6.04 (2H, m), 4.8 (2H, s), 3.80 (6H, s), 3.79 (3H, s); ^{13}C NMR (100 MHz, $CDCl_3$) δ: 169.4, 167, 164.4 (2C),160.1 (2C), 131.4, 131.3, 128.5, 119.7, 111.4, 104.5, 104.2, 103.6, 90.4 (2C), 55.5 (2C), 55.4, 37.8; EIMS m/z: 421.11; HPLC (% purity): 99%, $t_{r'}$ = 15.11.

*4.1.5.6. 3-(4-Fluorobenzyl)-5-(E/Z)(2,4,6-trimethoxybenzylidene)-1,3-thiazolidine-2,4-dione (**11f**).* (60 mg, 55%) yellow solid; Mpt. 166 °C; R_f 0.80 (50% EtOAc–hexane); ^{1}H NMR (400 MHz, $CDCl_3$) δ: 8.14 (1H, s), 7.38 (1H, d, J = 5.3 Hz), 7.34 (1H, d, J = 5.3 Hz), 6.92 (2H, d, J = 8.9 Hz), 6.04 (2H, m), 4.76 (2H, s), 3.8 (6H, s), 3.79 (3H, s); ^{13}C NMR (100 MHz, $CDCl_3$) δ: 167.1, 164.3, 163.7, 160.1 (2C), 131.6 (2C), 130.8, 130.7, 128.3, 120, 115.5, 115.3, 104.5, 90.4 (2C), 55.5 (2C), 55.4, 44; EIMS m/z: 403.07; HPLC (% purity): 99%, $t_{r'}$ = 15.17.

*4.1.5.7. 3-(4-Trifluoromethylbenzyl)-5-(E/Z)(2,4,6-trimethoxybenzylidene)-1,3-thiazolidine-2,4-dione (**11g**).* (54 mg, 44%) yellow solid; Mpt. 191 °C; R_f 0.64 (50% EtOAc–hexane); ^{1}H NMR (400 MHz, $CDCl_3$) δ: 8.17 (1H, s), 7.52 (2H, d, J = 8.4 Hz), 7.48 (2H, d, J = 7.6 Hz), 6.04 (2H, m), 4.85 (2H, m), 3.8 (6H, s), 3.79 (3H, s); ^{13}C NMR (100 MHz, $CDCl_3$) δ: 169.4, 166.9, 164.5, 160.2 (2C), 139.6, 129.6, 128.5 (2C), 125.5, 125.4 (2C), 119.8, 104.6, 90.6 (2C), 55.4 (3C), 44.2; EIMS m/z: 453.07; HPLC (% purity): 99%, $t_{r'}$ = 16.01.

*4.1.5.8. 3-(3-Methoxybenzyl)-5-(E/Z)(2,4,6-trimethoxybenzylidene)-1,3-thiazolidine-2,4-dione (**11h**).* (48 mg, 42%) yellow solid; Mpt. 158 °C; R_f 0.56 (50% EtOAc–hexane); ^{1}H NMR (400 MHz, $CDCl_3$) δ: 8.14 (1H, s), 7.14 (1H, t, J = 7.9 Hz), 6.95–6.91 (2H, m), 6.75 (1H, dd, J = 2.5, 8.2 Hz), 6.02 (2H, m), 4.76 (2H, m), 3.79 (6H, s), 3.78 (3H, s), 3.72 (3H, s); ^{13}C NMR (100 MHz, $CDCl_3$) δ: 169.6, 167.1, 164.2, 160.1 (2C), 159.7, 151.5, 137.2, 129.6, 128.1, 121, 114.2, 113.6, 104.6, 90.4 (2C), 55.5 (2C), 55.4, 55.2, 44.7; EIMS m/z: 415.08; HPLC (% purity): 99%, $t_{r'}$ = 15.12.

*4.1.5.9. 3-Adamentyl-5-(2,4,6-trimethoxybenzylidene)-1,3-thiazolidine-2,4-dione (**11i**).* (60 mg, 51%) yellow solid; Mpt. 272 °C; R_f 0.68 (5% IPA–DCM); ^{1}H NMR (400 MHz, DMSO) δ: 7.87 (1H, s), 6.28 (2H, m), 3.83 (9H, s), 2.30–1.67 (15H, m); ^{13}C NMR (100 MHz, DMSO) δ: 169.7, 168.7, 164.6, 160 (2C), 126.2, 122.2, 103.6, 90.5 (2C), 56.1 (3C), 49.3, 39.6 (3C), 35.3 (3C), 32.6 (3C); EIMS *m/z*: 429.07; HPLC (% purity): 99%.

4.2. Evaluation of in vitro antiplasmodial activity

4.2.1. Enzyme inhibition

Falcipain-2 was recombinantly expressed in *Escherichia coli* and refolded to the active enzyme as previously described [33]. IC_{50} values against recombinant falcipain-2 was determined as follows. The substrate ($H\text{-}_D$-Val-Leu-Arg-AFC), added to a final concentration of 30 μM for FP-2, was mixed at room temperature with different concentrations of tested inhibitors in the reaction buffer (100 mM sodium acetate, pH 5.5, 500 μM CHAPS, and 10 mM DTT). Inhibitor solutions were prepared from stocks in DMSO (maximum concentration of DMSO in the assay was 1%).

The reaction was started with the addition of the 0.25 nM FP-2 recombinant enzyme. Fluorescence was monitored for 1 h at room temperature in a SpectraMax Plus 384 spectrofluorometer. IC_{50} values were determined from plots of percent activity over concentration using GraFit software.

4.2.2. Cultured malaria parasites inhibition

The effects of inhibitors were studied against W2-strain *P. falciparum*, obtained from the Malaria Research and Reference Reagent Resource Center and cultured with human erythrocytes at 2% haematocrit in RPMI medium with either 10% human serum or 0.5% AlbuMAX II serum substitute. Synchrony was maintained with sorbitol. Cultures were incubated with serial dilutions of test compounds from 1000× stocks in DMSO for 48 h beginning at the ring stage. The medium was changed after 24 h, with maintenance of the appropriate inhibitor concentration. After 48 h, when control cultures contained nearly all new ring-stage parasites, parasites were fixed with 1% formaldehyde in PBS, pH 7.4, for 48 h at room temperature and then labelled with YOYO-1 (1 nM; Molecular Probes) in 0.1% Triton X-100 in PBS. Parasitaemias were determined from dot plots (forward scatter vs fluorescence) acquired on a FACSort flow cytometer using CELLQUEST software (Becton Dickinson). IC_{50} values for growth inhibition were determined with GraphPad Prism software from plots of percentage parasitaemia compared to controls (untreated parasites) over inhibitor concentration. In each case, the goodness of curve fit was documented by R^2 values of $\geq$0.95.

4.3. Molecular modelling studies

4.3.1. Protein structure preparation

Four crystal structures are available for FP-2: 3BPF (FP-2 covalently linked to E64 at 2.9 Å resolution) [34], 1YVB (FP-2 covalently linked to cystatin at 2.7 Å resolution) [35], 2GHU (not complexed at 3.1 Å resolution) [36] and 2OUL (FP-2 covalently linked to chagasin at 2.2 Å resolution) [37]. Although both 1YVB and 2OUL had better resolution than 3BPF, they are complexed to large inhibitors (over 100 amino acids). In contrast, 3BPF contains E64, a low molecular-weight, non-selective inhibitor that is comparable to our class of compounds. The protein was prepared using the Protein Preparation Wizard incorporated in Maestro [38] by adding missing hydrogen and side chains. All co-crystallised water molecules and bad contacts were removed. The receptor grid generation tool on Glide 5.7 was used to generate grid maps that covered the target's active site and the grid centres were defined by the co-crystallised ligand E64.

4.3.2. Ligand preparation and docking

To validate our docking calculations, non-covalent docking experiments were performed using E64 with the epoxide ring opened. ConfGen version 2.3, on Maestro, generated different conformations of the E64 and compound **9i**, which were later docked into the target, FP-2. In the docking process, standard-precision (SP) and extra-precision (XP) docking calculations were respectively adopted with default Glide docking parameters to generate the minimized poses using 5000 energy minimisation steps. The Glide scoring function (G-Score) was used to select the final 5 poses for each ligand and the conformation with lowest binding score was selected. Maestro was used to view and analyze the best docked conformations.

4.4. Metabolite ID incubations

4.4.1. In vitro metabolism incubations

The test compound (10 μM) was incubated at 37 °C with a solution of human (pooled human mixed gender) or rat (male rat IGS) liver microsomes (Xenotech) and NADPH (1 mM) in phosphate buffer (100 mM, pH 7.4) which contained magnesium chloride (5 mM) for 1 h while shaking. An equal volume of ice cold acetonitrile was added to stop the reaction and to precipitate the proteins. After centrifuging the mixture at 14,000 rpm for 30 min the supernatant was transferred to an HPLC vial. Control samples with no NADPH, no microsomes and a T0 sample were also included and processed in the same manner.

4.4.2. Analysis

The samples were analysed using an Agilent 1200 Rapid Resolution (600 bar) HPLC, with a diode array detector, coupled to an AB SCIEX 4000 QTRAP MS (ABSciex, Johannesburg, South Africa). For elution, 0.1% formic acid in water (with 5% acetonitrile) and 0.1% formic acid in 95% acetonitrile were used as mobile phases A and B respectively. A Kinetex C_{18} (150 mm × 2.1 mm), packed with 2.6 μm fused-core particles (Separations, Johannesburg, South Africa) was used for the analysis. The gradient run from 0% to 90% B in 9 min, where it was held for 3 min, before re-equilibration to the starting conditions. The total run time was 15 min. The LC-MS method was created using Lightsight v2.1 (AB Sciex) which relied on Analyst v. 1.5 method files created during direct infusion of the compounds. The methods were in electrospray positive mode and consisted of full scans coupled through information dependent acquisition to two enhanced product ion scans. The scan range was 100–600 using a scan rate of 4000 Da/s giving a total cycle time of 1.02 s. Collision energy was set to 30 ± 15 for **1** and 40 ± 15 for **9**. The source temperature was 500 °C, ion spray voltage 5000 V and curtain gas 20 psi. The sheath gas (gas 1) and nebulizer gas (gas 2) were set to 50 psi.

An extra set of runs was done with the same set of conditions as above but passing the eluent through the diode array detector (DAD). An Ascentis C_{18} (150 mm × 4.6 mm) was used instead of the column above to reduce the system back pressure and allow DAD detection.

Metabolites were identified by comparison of sample and control runs using Lightsight v2.1. A neutral loss and precursor fragment filter was also used post-acquisition using the IDATrace Extractor script in analyst 1.5 to ensure that all parent derived peaks were detected. Comparing their fragmentation patterns to that of the parent compound tentatively identified the metabolites.

4.5. Cytotoxic assay

Test samples were screened for *in vitro* cytotoxicity against a mammalian cell-line, Chinese Hamster Ovarian (CHO) using the 3-(4,5-dimethylthiazol-2-yl)-2,5-diphenyltetrazoliumbromide (MTT)-assay. The MTT-assay is used as a colorimetric assay for cellular growth and survival, and compares well with other available assays [39] and [40]. The tetrazolium salt MTT was used to measure all growth and chemosensitivity. The test samples were tested in triplicate. The test samples were prepared to a 20 mg/ml stock solution in 100% DMSO. Test compounds were stored at −20 °C. Dilutions were prepared on the day of the experiment. Emetine was used as the reference drug in all experiments. The initial concentration of emetine was 100 μg/ml, which was serially diluted in complete medium with 10-fold dilutions to give 6 concentrations, the lowest being 0.001 μg/ml. The same dilution technique was applied to the test samples. The highest concentration of solvent to which the cells were exposed had no measurable effect on cell viability (data not shown). The 50% inhibitory concentration (IC_{50}) values were obtained from full dose–response curves, using a non-linear dose–response curve fitting analysis via GraphPad Prism v. 4 software.

Acknowledgements

The University of Cape Town, South African Medical Research Council, and South African Research Chairs Initiative of the Department of Science and Technology, administered through the South African National Research Foundation are gratefully acknowledged for support (K.C.).

Appendix A. Supplementary data

Supplementary data related to this article can be found at http://dx.doi.org/10.1016/j.ejmech.2014.11.061.

References

[1] World Health Organisation, World Malaria Report 2012, 2012. Geneva.
[2] J.N. Burrows, K. Chibale, T.N.C. Wells, The state of the art in anti-malarial drug discovery and development, Curr. Top. Med. Chem. 11 (2011) 1226–1254.
[3] F. Gamo, L.M. Sanz, J. Vidal, C. de Cozar, E. Alvarez, J. Lavandera, D.E. Vanderwall, D.V. Green, V. Kumar, S. Hasan, J.R. Brown, C.E. Peishoff, L.R. Cardon, J.F. Garcia-Bustos, Thousands of chemical starting points for antimalarial lead identification, Nature 465 (2010) 305–310.
[4] M.P. Anthony, J.N. Burrows, S. Duparc, J.J. Moehrle, T.N.C. Wells, The global pipeline of new medicines for the control and elimination of malaria, Malar. J. 11 (2012) 316.
[5] P.J. Rosenthal, P.S. Sijwali, A. Singh, B.R. Shenai, Cysteine proteases of malaria parasites: targets for chemotherapy, Curr. Pharm. Des. 8 (2002) 1659–1672.
[6] R. Oliveira, R.C. Guedes, P. Meireles, I.S. Albuquerque, L.M. Gonçalves, E. Pires, M.R. Bronze, J. Gut, P.J. Rosenthal, M. Prudencio, R. Moreira, P.M. O'Neill, F. Lopes, Tetraoxane-pyrimidine nitrile hybrids as dual stage antimalarials, J. Med. Chem. 57 (2014) 4916–4923.
[7] Y. Liu, W.-Q. Lu, K.-Q. Cui, W. Luo, J. Wang, C. Guo, Synthesis and biological activities of novel artemisinin derivatives as cysteine protease falcipain-2 inhibitors, Arch. Pharm. Res. 35 (2012) 1525–1531.
[8] U.R. Mane, H. Li, J. Huang, R.C. Gupta, S.S. Nadkarni, R. Giridhar, P.P. Naik, M.R. Yadav, Pyrido[1,2-*a*]pyrimidin-4-ones as antiplasmodial falcipain-2 inhibitors, Bioorg. Med. Chem. 20 (2012) 6296–6304.
[9] F. Shah, Y. Wu, J. Gut, Y. Pedduri, J. Legac, P.J. Rosenthal, M.A. Avery, Design, synthesis and biological evaluation of novel benzothiazole and triazole analogs as falcipain inhibitors, MedChemComm 2 (2011) 1201.
[10] F. Shah, P. Mukherjee, J. Gut, J. Legac, P.J. Rosenthal, B.L. Tekwani, M.A. Avery, Identification of novel malarial cysteine protease inhibitors using structure-based virtual screening of a focused cysteine protease inhibitor library, J. Chem. Inf. Model. 51 (2011) 852–864.
[11] S. Praveen Kumar, J. Gut, R.C. Guedes, P.J. Rosenthal, M.M.M. Santos, R. Moreira, Design, synthesis and evaluation of 3-methylene-substituted indolinones as antimalarials, Eur. J. Med. Chem. 46 (2011) 927–933.
[12] J.M. Coterón, D. Catterick, J. Castro, M.J. Chaparro, B. Díaz, E. Fernández, S. Ferrer, F.J. Gamo, M. Gordo, J. Gut, L. Heras, J. Legac, M. Marco, J. Miguel, V. Munoz, E. Porras, J.C. Rosa, J.R. Ruiz, P. Ventosa, P.J. Rosenthal, J.M. Fiandor, Falcipain inhibitors: optimization studies of the 2-pyrimidinecarbonitrile lead series, J. Med. Chem. 53 (2010) 6129–6152.
[13] A. Breuning, B. Degel, F. Schulz, C. Büchold, M. Stempka, U. Machon, et al., Michael acceptor based antiplasmodial and antitrypanosomal cysteine protease inhibitors with unusual amino acids, J. Med. Chem. 53 (2010) 1951–1963.
[14] J.N. Domínguez, C. León, J. Rodrigues, N. Gamboa de Domínguez, J. Gut, P.J. Rosenthal, Synthesis and evaluation of new antimalarial phenylurenyl chalcone derivatives, J. Med. Chem. 48 (2005) 3654–3658.
[15] S. Batra, Y.A. Sabnis, J. Rosenthal, M.A. Avery, Structure-based approach to falcipain-2 inhibitors: synthesis and biological evaluation of 1,6,7-trisubstituted dihydroisoquinolines and isoquinolines, 11 (2003) 2293–2299.
[16] D.C. Greenbaum, Z. Mackey, E. Hansell, P. Doyle, J. Gut, C.R. Caffrey, J. Lehrman, P.J. Rosenthal, J.H. McKerrow, K. Chibale, Synthesis and structure–activity relationships of parasiticidal thiosemicarbazone cysteine protease inhibitors against *Plasmodium falciparum*, *Trypanosoma brucei*, and *Trypanosoma cruzi*, J. Med. Chem. 47 (2004) 3212–3219.
[17] P.S. Sijwali, P.J. Rosenthal, Gene disruption confirms a critical role for the cysteine protease falcipain-2 in hemoglobin hydrolysis by *Plasmodium falciparum*, Proc. Natl. Acad. Sci. U. S. A. 101 (2004) 4384–4389.
[18] E. Guantai, K. Ncokazi, T.J. Egan, J. Gut, P.J. Rosenthal, R. Bhampidipati, A. Kopinathan, P.J. Smith, K. Chibale, Enone- and chalcone-chloroquinoline hybrid analogues: *in silico* guided design, synthesis, antiplasmodial activity, *in vitro* metabolism, and mechanistic studies, J. Med. Chem. 54 (2011) 3637–3649.
[19] J. Lavrado, G.G. Cabal, M. Prudêncio, M.M. Mota, J. Gut, P.J. Rosenthal, C. Diaz, R.C. Guedes, D.V.J.A. Santos, E. Bichenkova, K.T. Douglas, R. Moreira, A. Paulo, Incorporation of basic side chains into cryptolepine scaffold: structure–antimalarial activity relationships and mechanistic studies, J. Med. Chem. 54 (2011) 734–750.
[20] P. Gibbons, E. Verissimo, N.C. Araujo, V. Barton, G.L. Nixon, R.K. Amewu, J. Chadwick, P.A. Stocks, G.A. Biagini, A. Srivastava, P.J. Rosenthal, J. Gut, R.C. Guedes, R. Moreira, R. Sharma, N. Berry, M.L.S. Cristiano, A.E. Shone, S.A. Ward, P.M. O'Neill, Endoperoxide carbonyl falcipain 2/3 inhibitor hybrids: toward combination chemotherapy of malaria through a single chemical entity, J. Med. Chem. 53 (2010) 8202–8206.
[21] G. Mugumbate, A.S. Newton, P.J. Rosenthal, J. Gut, R. Moreira, K. Chibale, R.J. Guedes, Novel anti-plasmodial hits identified by virtual screening of the ZINC database, J. Comput. Aided Mol. Des. 27 (2013) 859–871.
[22] P.S. Kenderekar, R. Siddiqui, P. Patil, S. Bhusare, R. Pawar, Synthesis and antibacterial activity of Schiff bases and 4-thiazolidinones, Indian J. Pharm. Sci. 65 (2003) 313.
[23] P. Vicini, A. Geronikaki, K. Anastasia, M. Incerti, F. Zani, Synthesis and antimicrobial activity of novel 2-thiazolylimino-5-arylidene-4-thiazolidinones, Bioorg. Med. Chem. 14 (2006) 3859–3864.
[24] S. Wang, Y. Zhao, G. Zhang, Y. Lv, N. Zhang, P. Gong, Design, synthesis and biological evaluation of novel 4-thiazolidinones containing indolin-2-one moiety as potential antitumor agent, Eur. J. Med. Chem. 46 (2011) 3509–3518.
[25] N.H. Metwally, M.A. Abdalla, M.A.N. Mosselhi, E.A. El-Desoky, Synthesis and antimicrobial activity of some new *N*-glycosides of 2-thioxo-4-thiazolidinone derivatives, Carbohydr. Res. 345 (2010) 1135–1141.
[26] R. Ottanà, S. Carotti, R. Maccari, I. Landini, G. Chiricosta, B. Caciagli, M.G. Vigorita, E. Mini, *In vitro* antiproliferative activity against human colon cancer cell lines of representative 4-thiazolidinones. Part I, Bioorg. Med. Chem. Lett. 15 (2005) 3930–3933.
[27] V. Gududuru, E. Hurh, J.T. Dalton, D.D. Miller, Synthesis and antiproliferative activity of 2-aryl-4-oxo-thiazolidin-3-yl-amides for prostate cancer, Bioorg. Med. Chem. Lett. 14 (2004) 5289–5293.
[28] J. Balzarini, B. Orzeszko-Krzesińska, J.K. Maurin, A. Orzeszko, Synthesis and anti-HIV studies of 2- and 3-adamantyl-substituted thiazolidin-4-ones, Eur. J. Med. Chem. 44 (2009) 303–311.
[29] S. Kamila, H. Ankati, E.R. Biehl, Microwave assisted synthesis of novel functionalized hydantoin derivatives and their conversion to 5-(*Z*) arylidene-4*H*-imidazoles, Molecules 16 (2011) 5527–5537.
[30] R.A. Friesner, R.B. Murphy, M.P. Repasky, L.L. Frye, J.R. Greenwood, T.A. Halgren, et al., Extra precision glide: docking and scoring incorporating a model of hydrophobic enclosure for protein–ligand complexes, J. Med. Chem. 49 (2006) 6177–6196.
[31] Glide, Version 5.7, Schrödinger L.L.C., New York, 2011. http://www.schrodinger.com.
[32] C. Teixeira, J.R.B. Gomes, P. Gomes, Falcipains, *Plasmodium falciparum* cysteine proteases as key drug targets against malaria, Curr. Med. Chem. 18 (2011) 1555–1572.
[33] P.S. Sijwali, L.S. Brinen, P.J. Rosenthal, Systematic optimization of expression and refolding of the *Plasmodium falciparum* cysteine protease falcipain-2, Protein Expr. Purif. 22 (2001) 128–134.
[34] I.D. Kerr, J.H. Lee, K.C. Pandey, A. Harrison, M. Sajid, P.J. Rosenthal, L.S. Brinen, Structures of falcipain-2 and falcipain-3 bound to small molecule inhibitors: implications for substrate specificity, J. Med. Chem. 52 (2009) 852–857.
[35] S.X. Wang, K.C. Pandey, J.R. Somoza, P.S. Sijwali, T. Kortemme, L.S. Brinen, et al., Structural basis for unique mechanisms of folding and hemoglobin binding by a malarial protease, Proc. Natl. Acad. Sci. U. S. A. 103 (2006) 11503–11508.
[36] T. Hogg, K. Nagarajan, S. Herzberg, L. Chen, X. Shen, H. Jiang, et al., Structural and functional characterization of falcipain-2, a hemoglobinase from the

malarial parasite *Plasmodium falciparum*, J. Biol. Chem. 281 (2006) 25425–25437.
[37] S.X. Wang, K.C. Pandey, J. Scharfstein, J. Whisstock, R.K. Huang, J. Jacobelli, R.J. Fletterick, P.J. Rosenthal, M. Abrahamson, L.S. Brinen, A. Rossi, A. Sali, J.H. Mckerrow, The structure of chagasin in complex with a cysteine protease clarifies the binding mode and evolution of an inhibitor family, Structure 15 (2007) 535–543.
[38] Maestro, Version 9.3, Schrödinger, LLC, New York, NY, 2012. http://www.schrodinger.com.
[39] T. Mosmann, Rapid colorimetric assay for cellular growth and survival: application to proliferation and cytotoxicity assays, J. Immunol. Methods 65 (1983) 55–63.
[40] L.V. Rubinstein, R.H. Shoemaker, K.D. Paull, R.M. Simon, S. Tosini, P. Skehan, D.A. Scudiero, A. Monks, M.R. Boyd, Comparison of *in vitro* anticancer-drug-screening data generated with a tetrazolium assay versus a protein assay against a diverse panel of human tumor cell lines, J. Natl. Cancer Inst. 82 (1990) 1113–1118.